Appl. Phys. A 81, 1533–1538 (2005)
DOI: 10.1007/s00339-005-3391-1

Applied Physics A
Materials Science & Processing

O.I. SHKLYAREVSKII[1,2]
S. SPELLER[1]
H. VAN KEMPEN[1,✉]

Conductance of highly oriented pyrolytic graphite nanocontacts

[1] Institute for Molecules and Materials, Radboud University Nijmegen, Toernooiveld 1, 6525 ED Nijmegen, Netherlands
[2] B. Verkin Institute for Low Temperature Physics & Engineering, National Academy of Science of Ukraine, 47 Lenin Av., 61103, Kharkov, Ukraine

Received: 15 April 2005/Accepted: 23 August 2005
Published online: 27 September 2005 •

ABSTRACT The conductance-voltage $G(V)$ characteristics for contacts between electrodes of highly oriented pyrolytic graphite were studied in a wide range of $G(0)$, bias voltages, and temperatures using the mechanically controllable break junction technique. Our results show a striking resemblance to corresponding data for conducting multiwall carbon nanotubes. For high-ohmic contacts between a single or a few graphene sheets, zero bias anomalies related to strong *e–e* Coulomb interactions and quantum interference of electrons is observed.

PACS 72.15.-v.; 72.80.Rj; 73.63.Rt

1 Introduction

The renewed interest in the conducting properties of graphite and highly oriented pyrolytic graphite (HOPG) in particular, was stimulated by the latest advances in investigation of carbon-based nanoscale devices. It was shown [1] that conductance versus voltage dependencies $G(V)$ of nanocontacts between liquid mercury and HOPG measured at room temperature is quite close to that of the contacts between Hg and multiwall carbon nanotubes (MWNTs). Very recent studies of atomically thin carbon films (few-layer graphene) [2] revealed the potential of this material for metallic transistor applications. The authors [2] noted that the on-off ratio of such transistors at room temperature may be considerably increased in a point-contact geometry. Moreover, the progress in producing ultrathin epitaxial graphite films [3] suggests a high feasibility of graphene based nanoelectronics. Such films can be patterned by oxygen plasma etching using well-developed lithographical processes [4].

Apart from [1] the only known attempt to measure the conductance of metal-graphite contacts was made by Agraït et al. [5] in an STM geometry by indenting the tungsten tip into the surface of HOPG. In both cases $G(V)$ curves were dominated by features due to the electron density of states .

In this article we are presenting a systematic study of the conductance of contacts between HOPG electrodes using the mechanically controllable break junction (MCBJ) technique. One of the main objectives was to explore the applicability of this method for the investigation of layered systems with HOPG as an illustrative example. Even though a great number of conducting materials with different mechanical and transport properties were explored using point-contacts and MCBJ in particular, it was not clear up to now whether reasonably reproducible results of any importance could be derived for this class of highly anisotropic conductors. It should be remembered that HOPG (or the stack of graphene planes) can be considered as a semimetal whereas an individual graphene sheet is a zero-gap metal. Another subject of interest was the effect of reduced dimensionality (point-contact geometry) and therefore high current density on the conductance of HOPG. The closeness of the electronic structure of graphene and conducting carbon nanotubes (CNTs) was an additional motivation for our experiments. The large body of available data for conducting CNTs was used for comparison with our results and for a more reliable interpretation.

2 Experiment

Over the last decade the MCBJ technique was developed to its stage of perfection for investigation of nanocontacts of conducting materials with different physical properties and is described elsewhere[6]. However, breaking of layered materials occurs in a quite different way than in metallic wires. Because of extremely strong sp^2 covalent intralayer bonds and relatively weak Van der Waals interlayer bonds in HOPG, the fracture and subsequent break of graphene sheets occurs individually and at random distances from the prearranged geometrical center of the junction. In this case the complete separation of electrodes (starting from the onset of breakage) requires their subsequent displacement ΔS to be as large as 3 to 10 microns, whereas in metals ΔS is of order of 10 nm.

For sample preparation we used 0.5 to 5 micron plates cleaved from a $10 \times 10 \times 1.2\,\mathrm{mm}^3$ *ZYB* crystal of HOPG. Strips 200–400 μm wide and 4–6 mm in length were cut with a razor blade and notched, leaving a 20–40 μm wide "neck" (Fig. 1a). We found that the break occurs at much smaller ΔS when the sample was notched along the folding lines (emerging during cleaving of the HOPG crystal or produced artificially by bending the HOPG strip). However, this method

✉ Fax: +31 24 365 21 90, E-mail: H.vanKempen@science.ru.nl

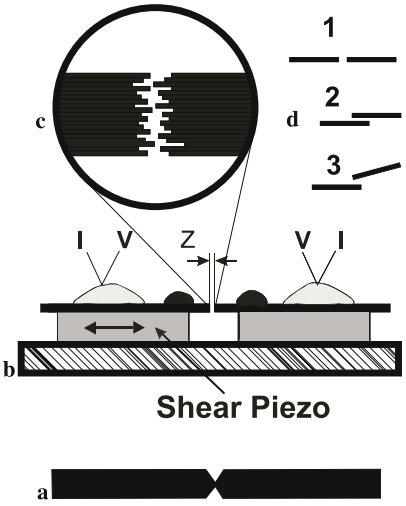

FIGURE 1 (**a**) Top view of the sample. (**b**) Modified sample mounting. The HOPG strip is glued on top of two shear piezo-ceramics attached to a phosphor bronze bending beam. The distance between the electrodes is controlled by vertically pushing the bending beam at the center or by applying voltage on the left-hand side shear piezo. All distances are exaggerated for clarity. (**c**) The suggested structure of the contact after the break. (**d**) Three possible types of individual contacts: 1 "end-to-end", 2 "side-to-side" and 3 "end-to-side"

drastically increases the density of defects in the electrodes and deteriorates conductance characteristics of the junction.

In our experiments with HOPG we used a somewhat modified version of the conventional sample mounting (Fig. 1b). It includes two identical pieces ($5 \times 2.5 \times 1\,\mathrm{mm}^3$) of shear piezoceramic (that gives a horizontal displacement of its surface upon applied voltage) placed underneath the anchoring points of the sample. The left-hand side piezo served for the fine adjustment of the contact conductance. Also, the distance between the electrodes can be tuned by changing the substrate deflection. This type of the sample mounting practically does not affect the junction stability.

Low temperature experiments were performed in cryogenic vacuum at $T \sim 5$–6 K, in He exchange gas and liquid He at 4.2 K or in superfluid He at 1.2 K. The most stable and reproducible results were obtained in He exchange gas. The large power dissipated in the low-ohmic junctions at high bias voltages (up to 10–100 mW) and the subsequent local overheating, resulted in instabilities in contact conductance when measured in liquid He. Part of the measurements were done at 77 and 300 K, with an excess pressure of He exchange gas in the cryostat to avoid contamination of electrodes and to preclude the possible influence of surfactant on the junction conductance.

The conductance of the HOPG MCBJ was measured using a Keithley 2400 SourceMeter in the range from ≈ 100 to $10^{-5}\,\mathrm{G}_0 (= 2e^2/h)$. Electrical leads to the strip of HOPG were attached either with silver paint or EPO-TEK 21D hard conducting epoxy. As the total resistance of contacts and external wiring (at 4.2 K) was usually less than 4–6 Ohm the two terminal method was sufficiently accurate in most of the cases.

In the layered materials we can expect three different types of contacts. In terms accepted for contacts between nanotubes they can be labelled as "end to end", "end to side (body)" (due to the unavoidable deformation in the course of breakage and subsequent connection and disconnection of the electrodes), and "side to side" contacts (see Fig. 1d).

The proportion between those types of contacts is unknown as well as their contribution into contact conductance. Whereas due to the high anisotropy of resistivity in HOPG (c-axis resistivity is four to five orders of magnitude higher than that in basal plane) the conductance of the "end to end" and "end to side" contacts is much higher, the total area of "side to side" contacts can be large enough to make an essential contribution into the overall $G(V)$ behavior. In spite of this fact we found more than sufficient reproducibility of conductance curves for contacts with conductance $\geq 1G_0$. For highly resistive junctions ($G \leq 0.1G_0$) the variation of the shape and amplitude of anomalies around zero bias was controlled for the most part by the specific distribution of the lattice defects. Nevertheless, even in this case all curves fall into very well defined categories. The reliability of the results discussed below is ensured by careful analysis of approximately 2000 conductance curves for more than 20 different samples.

3 Results and discussion

Conductance versus voltage dependencies $G(V)$ for HOPG MCBJ are changing gradually, along with an increase of the contact resistance or decrease of its effective size. Due to the overcomplicated multi-contact structure of graphite-graphite junctions, it is practically impossible to make a quantitative estimation of the contact diameter using the Sharvin formula [7] in the case of quasiballistic transport or the Wexler interpolation [8] for the diffusive regime of the current flow. In addition, we found that all $G(V)$ curves are quite similar within the three conventional ranges of zero-bias contact conductance $G(0)$: 1) 30–300 G_0, 2) 1–30 G_0 and 3) $G \leq 1G_0$.

The typical $G(V)$ curves for the first group are presented in Fig. 2. In the narrow interval of ± 200 mV the contact con-

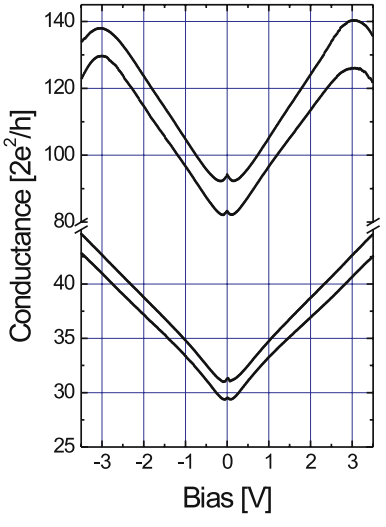

FIGURE 2 Conductance $G = I/V$ as a function of voltage for low-ohmic graphite-graphite MCBJ. The structure around zero bias is related to electron-phonon interaction. The origin of the maxima at approximately $V = 3$ V is discussed in the text

ductance decreases and afterwards increases practically linearly up to the limiting voltage of 3.5–4.0 V that we were able to attain without junction failure or up to its maximum around 3.0 V. The initial reduction of the junctions conductance can be explained by the strong electron–phonon interaction in graphite. The recent inelastic tunneling spectroscopy measurements of HOPG phonon spectrum [9] revealed features in the range from 5 meV (rigid layer shear mode) to 200 meV (optical modes). This interval is in a good agreement with our observations. However, we were not able to extract more detailed information (pronounced steps in conductance or singularities in the point-contact spectra $\mathrm{d}^2I/\mathrm{d}V^2$). This is not surprising taking into consideration the complex nature of our junctions resulting in smearing of the singularities in the point-contact spectrum [10]. The initial decrease in the junction conductance can be considered as proof of a quasi-ballistic or diffusive regime. This means that the inelastic electron mean free path is much larger than the typical contact "diameter" and can be roughly estimated as being of order of 10 microns or the average domain size in HOPG.

The subsequent linear behavior of conductance in the range 0.5–3.5 V is related to the linear increase in electron density of states in HOPG (see [11] and references therein) or graphene. The origin of maxima at some curves for low-ohmic contacts is not completely understood yet. Similar curves were observed for MWNTs with maxima around 2 V [1]. Current saturation and conductance maxima at much higher bias voltage (≈ 6 V) was reported in [12] although in this case the MWNTs most probably were semiconducting. At the same time data for MWNTs presented in [13] show no deviation from linearity in the range up to 3.5 V just like the conductance curves $G(V)$ for Hg-HOPG junctions. In [1] the conductance maxima were ascribed to properties of the liquid metal to nanotube contact rather then to intrinsic properties of the nanotube. On the other hand the early calculations of the electronic structure of graphite [14] predicted a V-shaped increase in density of states around the Fermi level culminating in maxima separated by 3.8–4.7 eV. More recent calculations of the electronic density of states for graphene [15], however, are placing these maxima at approximately ± 3.0 eV in much better agreement with our findings. This effect was observed only for junctions with the highest conductance we were able to measure. It should be noted that in spite of a very high power dissipation of ≥ 100 mW (the largest ever reported in point-contacts) the contacts remain remarkably stable.

Some of the contacts in this range of G do not display the conductance maximum around zero bias, but a monotonic increase in G with voltage. These contacts are considerably less stable and show the linear behavior of $G(V)$ only in a limited range of the bias voltages (usually ± 1.5–2.0 V). At higher voltage these curves demonstrate either successive series of sudden jumps to states with higher conductance or a rapid nonlinear growth of $G(V)$ until the limiting value of the current for the Keithley 2400 (105 mA) is reached. Continuously recording $G(V)$ dependencies displays a clear hysteretic behavior. This indicates a considerable overheating and thermal expansion of electrodes due to the gradual transition of the contact from the diffusive regime of the current flow to the so-called thermal limit with both elastic and inelastic mean free path of electrons smaller than the contact characteristic dimension. However the $G(V)$ curves at lower bias are fairly reproducible or show insignificant changes in the zero-bias conductance. This indicates that overheating of contacts is significantly lower than predicted for the "true" thermal limit: $eV = 3.63k_{\mathrm{B}}T$ [10]. This is because of the high thermal conductance of HOPG and the ever increasing contact diameter due to the thermal expansion of electrodes. (At $V_{\mathrm{b}} = 1$ V the temperature calculated from above formula reaches 3000 K, while graphene sheets are burned already around 1000 K.) It should be noted that for moderately overheated contacts we still anticipate a nearly linear $G(V)$ behavior. The linear increase of conductance of 2D graphene sheets with T was predicted in [16] and found experimentally for MWNTs in [17]. The latter result is expected because of crossover between the electron band structure of MWNTs and graphene at high temperatures.

Further decrease in $G(V_0)$ (range 1–$30\,G_0$) results in the emerging of a pronounced minimum around zero bias and strong deviation from linearity of $G(V)$ within an interval as large as ± 0.3–0.5 V (Fig. 3). The amplitude A of the minima can differ by a factor of 1.5–2.0 for contacts with the same G at $V = 1$ V. The general trend is increasing of A as the conductance decreases. The ultimate voltage reachable without a contact failure decreases to 2.5–3.0 V for contacts with $G(V_0) \approx 10G_0$ and 2.0–2.5 V for contacts with $G(V_0) \approx 1G_0$. However, while failure for the first group of contacts mostly results in an irreversible increase in zero-bias conductance, for the second group a sudden jump to a state with conductance below $1G_0^{-5}$ occurs. In the latter case a complete disconnection of electrodes happens as a result of "burning" of graphene sheets, in the same fashion that it occurs for the outermost part of MWNTs [1]. Usually it takes 1 to 3 nm of the shear piezo displacement to reestablish conductance of the junction at the original level.

Junctions with a zero-bias conductance below $1G_0$ (range 3, $G \leq 1G_0$), may be still multi-contact with a limited number of individual graphene layers participating in the

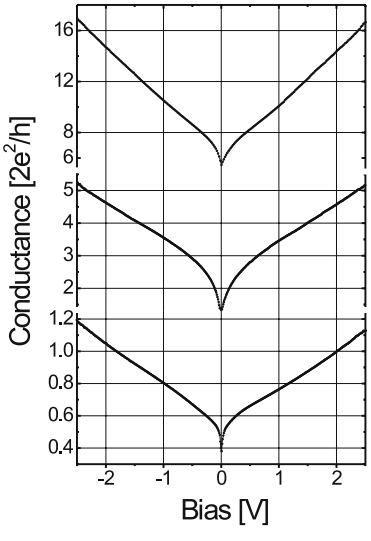

FIGURE 3 Conductance $G(V)$ versus V for the graphite–graphite junction with $G(0)$ in the intermediate range of 0.5–$10\,G_0$

conductance, or they may consist of a single contact for the most high-ohmic junctions. They show a very deep minimum or even a drop in conductance below $1G_0^{-5}$ (upper panel in Fig. 4) at $V \pm 10$–20 mV with a steep rise outside this interval. For these contacts failure takes place already at 1.0–1.5 V.

The overall behavior of the third group of the contacts discussed above (developing of conductance anomaly at low bias voltages, contact failure at relatively low V_b for high-ohmic contacts) suggests that the influence of lattice defects on conductance greatly increases as the contact dimension decreases. In other words, the concentration of defects along the contact axis peaks around the breaking line of graphene sheets. Such a distribution of defects is not uncommon for other semimetallic point-contacts. While low-ohmic contacts of Sb are ballistic, the high-ohmic junctions show the conductance anomalies typical for weak localization of charge carriers [18]. In our case the density of defects in a given contact is determined by the sample preparation history (HOPG crystal cleaving, notch production) and other ill-controlled details of the break of the neck. We believe that these factors are mainly responsible for the observed scattering of the data, especially for low conducting MCBJ.

Strong nonlinear behavior of $G(V)$ at low bias voltages was observed in point-contacts of various conducting materials elsewhere [19], and was ascribed to the different mechanisms of interaction of conducting electrons with two-level fluctuators (TLF) [20, 21]. However, the magnitude of zero-bias anomalies (ZBAs) in this case is rather small: less than 1% in metallic point-contacts and $\approx 5\%$ in highly disordered amorphous systems. In addition the energy range of these ZBAs is limited to approximately ± 10 mV.

Sharp drops in conductance at low bias voltages and low temperatures are a very usual phenomenon for single- and multiwall carbon nanotubes. To explain the origin of ZBAs

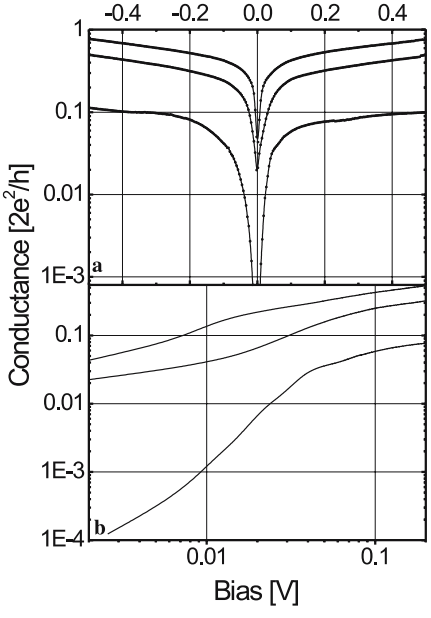

FIGURE 4 (**a**) Zero bias anomaly in conductance of the high-Ohmic graphite-graphite MCBJ. (**b**) The same curves as in upper panel in a double log scale

numerous models were put forward. For the single wall nanotubes the ZBA could be explained by Luttinger liquid (LL) behavior of highly correlated electrons in 1D conductors. It was proven by scaling of $G(V)$ dependencies taken at different temperatures into the universal curve [22, 23]. This model must be discarded in our case for the following reasons. Although in some cases (e.g. single atomic chain in Au or Pt MCBJ [24]) the dimensionality of the point-contact can be really reduced to 1D, the contact between graphene sheets most probably remains a 2D conductor. For high-ohmic junctions the electron transport is diffusive and the shape of the ZBA differs strongly from contact to contact, and does not comply with the power-law behavior predicted by the LL model (see lower panel in Fig. 4 and discussion below).

In the multiwall nanotubes the situation is far more complicated and is still the subject of debate. There are sufficiently strong reasons to explain the ZBA in terms of quantum interference of electron waves in the diffusive regime (2D weak localization) inherent to conventional Fermi liquid behavior [25, 26]. On the other hand some results still indicate unconventional features of the electron system [27, 28]. This complicated behavior most probably can be explained by interplay between a strong electron–electron Coulomb repulsion and electron–disorder scattering [29, 30].

Weak localization of electrons occurs in disordered conductors when the coherence length L_Θ is much larger than the elastic mean free path of electrons. At elevated temperatures the electron-phonon interaction is destroying the weak localization by decreasing the coherence length. Sufficiently high magnetic fields result in dephasing of electrons and reducing the ZBA amplitude. Therefore, the usual way to prove the validity of the weak localization model is to measure $G(T)$ and $G(H)$ dependencies. Unfortunately the drawback of MCBJ technique is the virtual impossibility of making temperature and magnetic field scans without noticeable changes of junction parameters. In the first case the difference of expansion coefficient in materials used in the sample mounting, results in a mechanical shift of electrodes. In the case of the magnetic field the residual magnetism in some parts of the insert, leads in most occasions to irreversible changes in the contact conductance. However, measurements of the contact conductance at any stable temperature in the range 1.2–300 K are still possible as well as the measurement of $G(V)$ in fixed magnetic fields.

Although for some contacts the remnants of very smeared ZBAs can still be observable even at 77 K, the typical set of $G(V)$ dependencies at this temperature usually shows no visible singularities at low bias voltages and a linear increase in conductance at elevated V_b (see upper panel in Fig. 5). At 300 K our results were practically identical to the data for Hg-HOPG contacts presented in [1].

The reproducible measurements of the contact conductance in a magnetic field perpendicular to the current flow direction were only possible for contacts with $G \geq 1G_0$. The pronounced ZBA remains practically unchanged in the magnetic field up to 5 T (lower panel in Fig. 5). This can be explained by the complex structure of contacts in layered conductors, making dephasing of electrons non-effective. Similar behavior of the ZBA in a magnetic field was observed by Lu et al. [28] for MWNTs. Following [28], we can suggest that

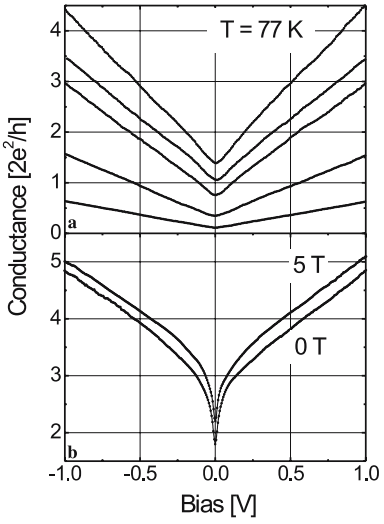

FIGURE 5 (**a**) Conductance $G(V)$ versus V for the graphite-graphite junction at 77 K (note the absence of ZBA). (**b**) $G(V)$ dependencies in a zero magnetic field and at $H = 5$ T

a substantial contribution to ZBA is originating from strong *e-e* interaction in 2D graphene (Coulomb gap).

However, the role of electron scattering should not be underestimated. The influence of rearrangement of the scattering centers on ZBA is shown in the upper panel in Fig. 6 for a series of five successive $G(V)$ curves measured for high-ohmic contact. At bias voltages exceeding 0.3–0.4 V the conductance of the contacts jumps between two or more levels creating the typical pattern of "telegraph noise" on the time scale of seconds (see inset in upper panel of Fig. 6). The latter effect occurs due to the electromigration of scattering centers within the contact and is not uncommon in disordered materials. This motion of defects was observed e.g. in metallic glasses where rearrangement of large "slow" defects affected the zero-bias peak related to the fast-switching two level fluctuators [19]. In superconducting NiNb contact fluctuations of large defects resulted in considerable changes of superconducting gap parameters [31]. High current density in graphite junctions at elevated bias voltages (estimated safely as being at least 10^7 A/cm^2) may lead to the motion of such defects as dislocations under the "electronic wind" forces. Whereas the change in conductance ΔG at ≈ 0.4 V is of order of 3 to 5%, the effect of redistribution of scattering centers on the shape and amplitude of the zero-bias anomaly is quite dramatic and indicates the essential role of electron scattering in agreement with the weak localization model. It should be noted that in the case that defects are pinned (or alternatively the concentration of the scattering centers is low) and no visible changes in the conductance occur at high bias voltages, the shape of the ZBA remains practically unchanged during multiple voltage scans (lower panel in Fig. 6). It is interesting that for these curves the conductance drops exponentially below $V_b < 200$ mV (see inset in lower panel in Fig. 6).

Approximately 5 to 10% of all curves for junctions with a low conductance show a more complicated behavior of conductance around zero bias with two local maxima in the range $\pm$20–40 mV (Fig. 7). Such behavior of $G(V)$ can be ascribed to the Coulomb blockade of electrons, and was reported in the contacts between crossed carbon nanowires before [32]. Normally this effect can be easily observed in the three electrode configuration provided that there is a sufficiently small capacity of the middle electrode ($e^2/2C \gg kT$) and a small tunneling conductance $G_T \ll G_0$. In our case a similar situation is possible due to the complex structure of the contact and specific distribution of scattering centers. For example Coulomb blockade was observed in a multiwalled carbon nanotube island with nanotube leads [33]. Moreover, it was shown that Coulomb blockade can be observed in a single contact under a high impedance environment caused by weak localization [34]. At higher bias voltages the electron-phonon interaction destroys weak localization and hence only the first peaks (or Coulomb gap) can be seen. Some $G(V)$ curves of

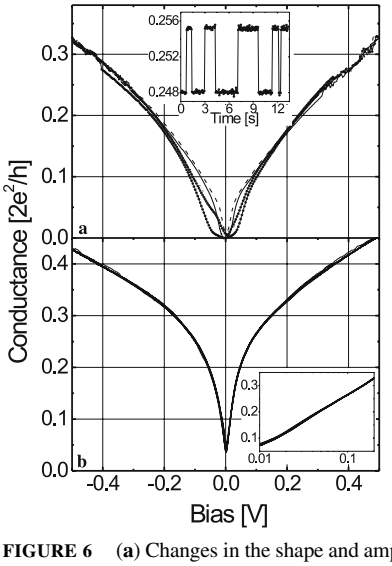

FIGURE 6 (**a**) Changes in the shape and amplitude of ZBA in the course of five successive measurement cycles. The rearrangement of defects at bias voltages $\geq$ 0.3–0.4 V results in different conditions for weak localization. *Inset*: "telegraph noise"-like behavior of conductance at V_b indicated by arrow. (**b**) In the case of pinned defects practically no changes in ZBA occur after 10 measurement cycles. *Inset*: $G(V)$ dependence on logarithmic scale

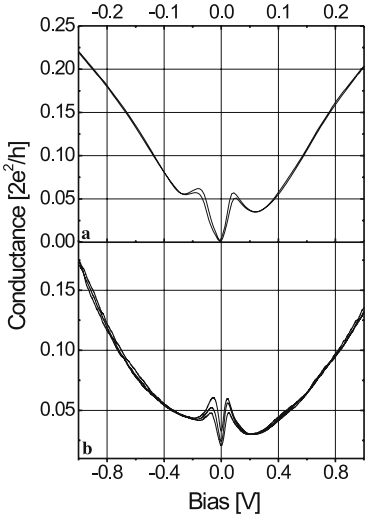

FIGURE 7 (**a,b**) Conductance $G(V)$ dependencies for high ohmic HOPG MCBJ displaying zero-bias behavior typical for Coulomb blockade

this type are more complicated (lower panel in Fig. 7). They have a finite conductance around $V = 0$ and a near quadratic dependence on V at elevated voltages. The latter indicates the presence of a substantial tunneling component in the contact conductance, probably due to parallel connected tunnel junctions.

4 Conclusion

In conclusion, we demonstrated the potential applicability of the MCBJ technique to highly anisotropic layered materials. The HOPG contact conductance can be considered as a sum of conductances of a large number of individual contacts between single graphene sheet or stacks of such sheets. This method can be refined by using HOPG samples with a thickness of ≈ 50–100 nm to facilitate breaking and minimization of the number of the structural defects. Predictably, low-ohmic contacts show better reproducibility than high-ohmic ones. At the high bias voltages the absolute majority of $G(V)$ curves are demonstrating nearly perfect linear behavior in accordance with the electron density of states both in HOPG crystals and graphene. The origin of the zero-bias anomalies in HOPG junctions is not quite clear. Most probably both strong $e-e$ Coulomb repulsion enhanced by the reduced dimensionality of the contacts and scattering of electrons by defects resulting in quantum interference effects are both contributing to this phenomenon.

ACKNOWLEDGEMENTS The authors are grateful to A. Toonen, J. Hermsen, and J. Gerritsen for invaluable technical assistance. Part of this work was supported by the stichting voor fundamenteel onderzoek der materie (FOM) which is financially supported by the nederlandse organisatie voor wetenschappelijk onderzoek (NWO). O.I.S. wishes to thank the NWO and FOM for visitor's grants.

REFERENCES

1 C. Berger, Y. Yi, J. Gezo, P. Poncharal, W.A. de Heer, New J. Phys. **5**, 158.1 (2003)
2 K.S. Novoselov, A.K. Geim, S.V. Morozov, D. Jiang, Y. Zhang, S.V. Dubonos, I.V. Grigorieva, A.A. Firsov, Science **306**, 666 (2004)
3 C. Berger, Z. Song, T. Li, X. Li, A.Y. Ogbazghi, R. Feng, Z. Dai, A.N. Marchenkov, E.H. Conrad, P.N. First, W.A. de Heer, arXiv: cond-mat/0410240v1
4 X. Lu, H. Huang, N. Nemchuk, R.S. Ruoff, Appl. Phys. Lett. **75**, 193 (1999)
5 N. Agraït, J.G. Rodrigo, S. Viera, Ultramicroscopy **42**, 177 (1992)
6 J.M. van Ruitenbeek, *Metal Cluster on Surfaces: Structure, Quantum Properties, Physical Chemistry*, K.H. Meiwes-Broer, ed. (Springer-Verlag, Heidelberg 2000) pp. 175–210; N. Agraït, A. Levy Yeyati, J.M. van Ruitenbeek, Phys. Reports. **377**, 8103 (2003)
7 Y.V. Sharvin, Sov. Phys. JETP **21**, 655 (1965)
8 A. Wexler, Proc. Phys. Soc. (London) **89**, 927 (1966)
9 L. Vitali, M.A. Schneider, K. Kern, L. Wirtz, A. Rubio, Phys. Rev. B **69**, 121 414 (2004)
10 Y.G. Naidyuk, I.K. Yanson, *Point Contact Spectroscopy* (Springer, New York 2004)
11 J.C. Boettger, Phys. Rev. B **55**, 11 202 (1997)
12 Y.X. Liang, Q.H. Li, T.H. Wang, Appl. Phys. Lett. **84**, 3379 (2004)
13 R. Hobara, S. Yoshimoto, T. Ikuno, M. Katayama, N. Yamamuchi, W. Wongwiriypan, S. Honda, I. Matsuda, S. Hasegawa, K. Oura, Jpn. J. Appl. Phys. **43**, L1081 (2004)
14 R.C. Tatar, S. Rabii, Phys. Rev. B **25**, 4126 (1982)
15 H. Terrones, M. Terrones, E. Hernandez, N. Grobert, J.C. Charlier, P.M. Ajayan, Phys. Rev. Lett. **84**, 1716 (2000)
16 J.C. Slonczewski, P.R. Weiss, Phys. Rev. **109**, 272 (1958)
17 F. Zhou, L. Lu, D.L. Zhang, Z.W. Pan, S.S. Xie, Solid. State. Commun. **129**, 407 (2004)
18 I.K. Yanson, O.I. Shklyarevskii, N.N. Gribov, J. Low Temp. Phys. **88**, 135 (1992)
19 R.J.P. Keijsers, O.I. Shklyarevskii, H. van Kempen, Phys. Rev. Lett. **77**, 3411 (1996); O.P. Balkashin, R.J.P. Keijsers, H. van Kempen, Y.A. Kolesnichenko, O.I. Shklyarevskii, Phys. Rev. B **58**, 1294 (1998)
20 V.I. Kozub, I.O. Kulik, Sov. Phys. JETP **64**, 1332 (1986)
21 K. Vladar, A. Zawadowski, Phys. Rev. B **28**, 1564 (1983); **28**, 1582 (1983); **28**, 1596 (1983)
22 M. Bockrath, D.H. Cobden, J. Lu, A.G. Rinzler, R.E. Smalley, L. Balents, P.L. McEuen, Nature **397**, 598 (1999)
23 Z. Yao, H.W.C. Postma, L. Balents, C. Dekker, Nature **402**, 273 (1999)
24 A.I. Yanson, G.R. Bollinger, H.E. van den Brom, N. Agraït, J.M. van Ruitenbeek, Nature **395**, 783 (1998)
25 A. Bachtold, C. Strunk, J.-P. Salvetat, J.-M. Bonard, L. Forro, T. Nussbaumer, C. Schönenberger, Nature **397**, 673 (1999)
26 D. Mendoza, F. Morales, R. Escudero, Solid State Commun. **130**, 317 (2004)
27 A. Bachtold, M. de Jonge, K. Grove-Rasmussen, P.L. McEuen M. Buitelaar, C. Schönenberger, Phys. Rev. Lett. **87**, 166 801 (2001)
28 N. Kang, L. Lu, W.J. Kong, J.S. Hu, W. Yi, Y.P. Wang, D.L. Zhang, Z.W. Pan, S.S. Xie, Phys. Rev. B **67**, 033 404 (2003)
29 R. Egger, A.O. Gogolin, Phys. Rev. Lett. **87**, 066 401 (2001)
30 E.G. Mishchenko, A.V. Andreev, L.I. Glazman, Phys. Rev. Lett. **87**, 246 801 (2001)
31 A. Halbritter, O.Y. Kolesnychenko, G. Mihaly, O.I. Shklyarevskii, H. van Kempen, Phys. Rev. B **61**, 5846 (2000)
32 J.W. Park, J. Kim, K.H. Yoo, J. Appl. Phys. **93**, 4191 (2003)
33 N. Yoneya, E. Watanabe, K. Tsukagoshia, Y. Aoyagi, Appl. Phys. Lett. **79**, 1465 (2001)
34 J. Haruyama, I. Takesue, Y. Sato, Appl. Phys. Lett. **77**, 2892 (2000)